

Article

An Investigation of Iodovanadinite Wasteforms for the Immobilisation of Radio-Iodine and Technetium

Daniel J. Bailey ^{1,*} , Erik V. Johnstone ^{1,2} , Martin C. Stennett ¹ , Claire L. Corkhill ^{1,3} and Neil C. Hyatt ^{3,4}

¹ Immobilisation Science Laboratory, Department of Materials Science and Engineering, University of Sheffield, Sheffield S1 3JD, UK; m.c.stennett@sheffield.ac.uk (M.C.S.)

² Innovative Fuel Solutions, LLC, North Las Vegas, NV 89031, USA

³ School of Earth Sciences, University of Bristol, Bristol BS8 1RJ, UK

⁴ School of Mechanical and Materials Engineering, Washington State University, Pullman, WA 99164, USA

* Correspondence: d.j.bailey@sheffield.ac.uk

Abstract: ⁹⁹Tc and ¹²⁹I are two long-lived, highly soluble and mobile fission products that pose a long-term hazard. A proposed wasteform for the disposal of radio-iodine is iodovanadinite (Pb₅(VO₄)₃I), an apatite-structured vanadate. In this investigation, a suite of potential iodovanadinite wasteforms designed for the co-disposal of Tc and I or the sole disposal of I were synthesised via hot isostatic pressing (with Mo as a surrogate for Tc). It was found that direct synthesis from oxide and iodide precursors was possible using hot isostatic pressing (HIPing). Increasing overpressure during HIPing was found to improve the density of the final product. X-ray diffraction (XRD) and scanning electron microscopy (SEM) analyses indicated that the use of AgI as the source of iodine affected the formation of the target iodovanadinite phase and produced unfavourable phase assemblages. Here, we report the direct synthesis of Pb₅(VO₄)₃I in a single step by hot isostatic pressing.

Keywords: ceramic; iodine; technetium; immobilisation; radioactive; nuclear; waste



Citation: Bailey, D.J.; Johnstone, E.V.; Stennett, M.C.; Corkhill, C.L.; Hyatt, N.C. An Investigation of Iodovanadinite Wasteforms for the Immobilisation of Radio-Iodine and Technetium. *Ceramics* **2023**, *6*, 1826–1839. <https://doi.org/10.3390/ceramics6030111>

Academic Editors: Gilbert Fantozzi and Nicolas Clavier

Received: 25 July 2023

Revised: 18 August 2023

Accepted: 21 August 2023

Published: 24 August 2023



Copyright: © 2023 by the authors. Licensee MDPI, Basel, Switzerland. This article is an open access article distributed under the terms and conditions of the Creative Commons Attribution (CC BY) license (<https://creativecommons.org/licenses/by/4.0/>).

1. Introduction

Radioactive iodine isotopes are produced as by-products of the nuclear fission of uranium fuel during nuclear power production. During the reprocessing of spent nuclear fuel (SNF), iodine is liberated. Although many iodine isotopes are relatively short-lived (e.g., ¹³¹I, $t_{1/2} = 8$ days) ¹²⁹I has a half-life of 15.7 million years and poses a significant long-term hazard. Consequently, sequestering and immobilising radio-iodine to reduce its long-term environmental hazards are of particular importance. Volatilised iodine is removed using various off-gas technologies, including aqueous scrubs or silver-impregnated solid sorbents that react to form AgI [1–5]. Although it is possible to subsequently isolate iodine from these extractants, any wasteform that can directly handle AgI would be advantageous [6,7]. Further, ⁹⁹Tc, like ¹²⁹I, is a long-lived ($t_{1/2} = 211,000$ years) and highly soluble mobile fission product [8]. Technetium is a problematic element with regards to vitrification but may be extracted from SNF during reprocessing by careful modification of PUREX/UREX flowsheets or by head-end processes such as voloxidation [9–11]. This raises the possibility of producing a tailored wasteform for its safe disposal. Given the long half-lives of ⁹⁹Tc and ¹²⁹I, co-immobilisation of these two isotopes in a single, tailored wasteform would be conceptually advantageous.

Iodovanadinite (Pb₅(VO₄)₃I), sometimes referred to as lead iodoapatite, has been identified as a potential host matrix for the immobilisation of ¹²⁹I [12]. Iodovanadinite is closely related to the mineral vanadinite (Pb₅(VO₄)₃Cl) and its counterparts pyromorphite (Pb₅(PO₄)₃Cl) and mimetite (Pb₅(AsO₄)₃Cl), all members of the larger apatite mineral family, crystallising in the hexagonal spacegroup *P*6₃/*m* [13]. The corner-sharing PO₄ tetrahedra found in archetypal apatites may be replaced with larger structural units, such as VO₄ or AsO₄ tetrahedra. Substituting the PO₄ unit with larger structural units increases the

aperture of the tunnel sites and subsequently improves the incorporation of larger anions, such as iodide, within the wasteform [12–15]. Apatites containing the ReO_5 structural unit have also successfully been synthesised. Because Re exhibits similar chemistry as its lighter congener, Tc, and is frequently used as an inactive surrogate, such apatite phases demonstrate potential for the co-immobilisation of both iodine and technetium in a single matrix [14,16].

Although iodovanadinite has previously been successfully synthesised by a variety of methods, including spark plasma sintering (SPS) and microwave synthesis [12,17,18], the volatile nature of iodine greatly complicates the synthesis and consolidation of these compounds. High-temperature heat treatment in an open atmosphere results in considerable loss of the initial iodine inventory, and consequently, methods of sample preparation or consolidation that minimise volatilisation, e.g., hot isostatic pressing (HIP) or mechanochemical processing, are of great interest [19–23].

The existence of the closely related mineral phases vanadinite, pyromorphite and mimetite provides an indication that the framework structure is relatively durable in the environment and therefore worthy of consideration as a possible host phase for the geological disposal of radionuclides. Studies of synthetic iodovanadinite have found that the release of iodine from the structure may be affected by the pH of the leaching solution. Maddrell and Abraitis (2004) reported that, over the course of a 14-day leach test in alkaline media (pH 11, $SA/V = 1 \text{ cm}^{-1}$), the normalised release rate of iodine from samples of $\text{Pb}_5(\text{VO}_4)_3\text{I}$ was $1.5 \text{ g}\cdot\text{m}^{-2}\text{d}^{-1}$ and that the release of iodine was incongruent with the dissolution of the matrix [23]. Dissolution of a partially phosphate substituted composition ($\text{Pb}_{10}(\text{VO}_4)_{4.8}(\text{PO}_4)_{1.2}\text{I}_2$), reported by Audubert and Guy (2002), found that the initial release rate in deionised water at 90°C was $2.4 \times 10^{-3} \text{ g}\cdot\text{m}^{-2}\text{d}^{-1}$ and increased markedly when moving to increasingly acidic media [24]. It was again found that iodine release was incongruent with matrix dissolution.

In this investigation, iodovanadinite compositions in the $\text{Pb}_{5-x}\text{Ag}_x(\text{VO}_4)_{3-x}(\text{MoO}_4)_x\text{I}$ and $\text{Pb}_{4.5-x}\text{Ba}_x\text{Ag}_{0.5}(\text{VO}_4)_3\text{I}_{0.5}$ series were synthesised using HIP with the aim of producing wasteforms suitable for both the sole disposal of AgI and the co-disposal of iodine and technetium. The resulting materials were characterised by powder X-ray diffraction, scanning electron microscopy and thermal analysis techniques. Materials similar to the $\text{Pb}_{4.5-x}\text{Ba}_x\text{Ag}_{0.5}(\text{VO}_4)_3\text{I}_{0.5}$ series have previously been described but not fully characterised by Uno et al. (2004) [25]. Subsequently, Johnstone et al. reported unsuccessful synthesis attempts of $\text{Pb}_9\text{Ag}(\text{VO}_4)_6\text{I}$ and $\text{Ba}_9\text{Ag}(\text{VO}_4)_6\text{I}$ endmembers via reaction in sealed quartz tubes [26]. Our study of the $\text{Pb}_{4.5-x}\text{Ba}_x\text{Ag}_{0.5}(\text{VO}_4)_3\text{I}_{0.5}$ series was pursued with the aim of determining whether a combination of Pb/Ba in conjunction with HIPing would prove more successful. Incorporation of AgI in the $\text{Pb}_{5-x}\text{Ag}_x(\text{VO}_4)_{3-x}(\text{MoO}_4)_x\text{I}$ series was hypothesised to be charge balanced by the incorporation of Mo as the MoO_4^{2-} anion, with Mo effectively acting as a surrogate for Tc. Mo was selected for this purpose due to the similarities between Tc and Mo in chemistry and ionic radius (adjacent 5d transition metals, ionic radius $\text{Tc}^{7+} = 0.41 \text{ \AA}$ and ionic radius of $\text{Mo}^{6+} = 0.37 \text{ \AA}$ in four-fold co-ordination). The MoO_4^{2-} anion is of a different charge to the pertechnetate anion (TcO_4^-), which is evidently a limitation on the use of Mo as a Tc surrogate in this speciation; however, the counterpart TcO_4^2 , tetraoxotechnetate (VI), species is known [10]. It was recognised that Re, as a congener of Tc, is more commonly used as a surrogate for Tc. However, for the purpose of this exploratory study, Mo was selected as a more cost-effective surrogate since the chemistry and ionic size of Mo and Tc were considered sufficiently similar to provide useful insight for the intended purpose. Nevertheless, the results presented here should be considered insightful only in the context of the hypothesised solid solution behaviour and methodology, and appropriate caution should be exercised in extrapolating the behaviour of Mo to Tc.

2. Materials and Methods

Iodovanadinites were prepared by a solid-state reaction between PbO, V₂O₅, MoO₃, PbI₂, AgI and Ba₃(VO₄)₂ precursors using a hot isostatic press (HIP). Ba₃(VO₄)₂ was used to provide a suitable Ba precursor that would not evolve gas during the HIPing process. In the Pb_{5-x}Ag_x(VO₄)_{3-x}(MoO₄)_xI series (x = 0, 0.2, 0.4, 0.6, 0.8, 1.0), PbI₂ was incrementally replaced as the iodine source by AgI. In the Pb_{4.5-x}Ba_xAg_{0.5}(VO₄)₃I_{0.5} series (x = 0, 0.5, 1.0, 1.5, 2.0, 2.5), AgI was the sole iodine source. Precursors were mixed with cyclohexane to form a slurry and ball milled in yttria-stabilised zirconia pots with yttria-stabilised zirconia media using a Fritsch Pulverisette 6 for five periods of 3 min at 500 rpm, changing the direction of milling with each period. Consolidated samples were produced by HIP (American Isostatic Presses-630H HIP, Columbus, OH, USA) in C106 copper tubing (~1.5 g sample, 6.5 mm OD, 2 mm ID) for 4 h at a temperature of 800 °C with an overpressure of 100 MPa. A preliminary set of baseline Pb₅(VO₄)₃I samples was produced to study the effect of overpressure on consolidation by HIPing at overpressures of 5, 10, 25 and 100 MPa and was used as a basis for the processing conditions for subsequent syntheses. Our choice of synthesis conditions was guided by consideration of the appropriate temperature to achieve a solid-state reaction within the temperature stability field of Pb₅(VO₄)₃I [19] and the expected range of overpressure necessary to achieve densification and the elimination of inter-granular porosity.

Reacted materials were ground to a fine powder and characterised by powder X-ray diffraction (XRD). XRD was performed using a Bruker D2 Phaser diffractometer (Bruker, Coventry, UK) utilising Cu K α radiation, a Ni foil K β filter and a position-sensitive detector. Measurements were made at 10° < 2 θ < 70° with a step size of 0.02 increments and a scan rate of 1 s per step. Phase analysis was completed using DiffraSuite Eva V.3 (Bruker) software.

Consolidated materials were sectioned using a Buehler Isomet Low Speed Saw, and the microstructures were characterised by scanning electron microscopy (SEM) in combination with energy dispersive X-ray spectroscopy (EDX) using a Hitachi TM3030 SEM (Hitachi, Warrington, UK) equipped with a Bruker Quantax EDX. An accelerating voltage of 15 kV was used for imaging. EDX data was processed using Bruker Quantax software. Sectioned materials were prepared for SEM analysis by mounting in cold setting resin and polishing with SiC paper and progressively finer diamond pastes to an optical finish (1 μ m). Samples were sputter-coated with carbon to reduce surface charging effects.

To determine the behaviour of precursor powders during heating, samples were investigated by thermogravimetric analysis-mass spectrometry using a Netzsch TG449 F3 Jupiter with an integrated QMS 403 D Aëolos mass spectrometer (Netzsch, Wolverhampton, UK). Samples were heated at a rate of 20 °C min⁻¹ in an argon atmosphere up to a temperature of 800 °C. The mass loss of samples was recorded, and evolved species were analysed using a 64 channel QMS 403 D Aëolos mass spectrometer. We optimised the sensitivity of our analysis for iodine detection, and, therefore, it was not possible to make an accurate assessment of weight loss attribution to other evolved gases.

3. Results and Discussion

3.1. HIPing of Baseline Pb₅(VO₄)₃I and the Effect of Overpressure during Consolidation

Figures 1 and 2 show the results of X-ray diffraction and representative micrographs for baseline iodovanadinite (Pb₅(VO₄)₃I) consolidated at overpressures of 5, 10, 25 and 100 MPa, respectively. As can be seen in Figure 1, the iodovanadinite phase is formed under all overpressures; there is also evidence of the retention of a small amount of PbI₂. Although the applied overpressure does not have a major effect on the observed phase assemblage, it does have an effect on the final microstructure. Increasing overpressure results in improved densification and lower inter-granular porosity, yielding a superior wasteform relative to those produced with lower overpressures. An overpressure of 100 MPa was required to eliminate inter-granular porosity. It was not possible to make a more quantitative determination of porosity due to the preferential pull-out of PbI₂ grains during specimen

preparation for SEM analysis. It is also apparent from SEM (Figure 2) that, while not evident by XRD, a small proportion of V_2O_5 was retained (phases were determined by SEM-EDX mapping, see Figure 3; iodine-rich regions were assumed to be PbI_2 based on XRD results, thus differentiating them from iodovanadinite). Although iodovanadinite has previously been synthesised directly from oxides by mechanochemical processing followed by thermal annealing or spark plasma sintering [21,27], this represents the first reported instance of direct synthesis by hot isostatic pressing. The removal of the intermediate $Pb_3(VO_4)_2$ synthesis step reduces the number of necessary operations and is therefore a considerable simplification of the conceptual manufacturing process.

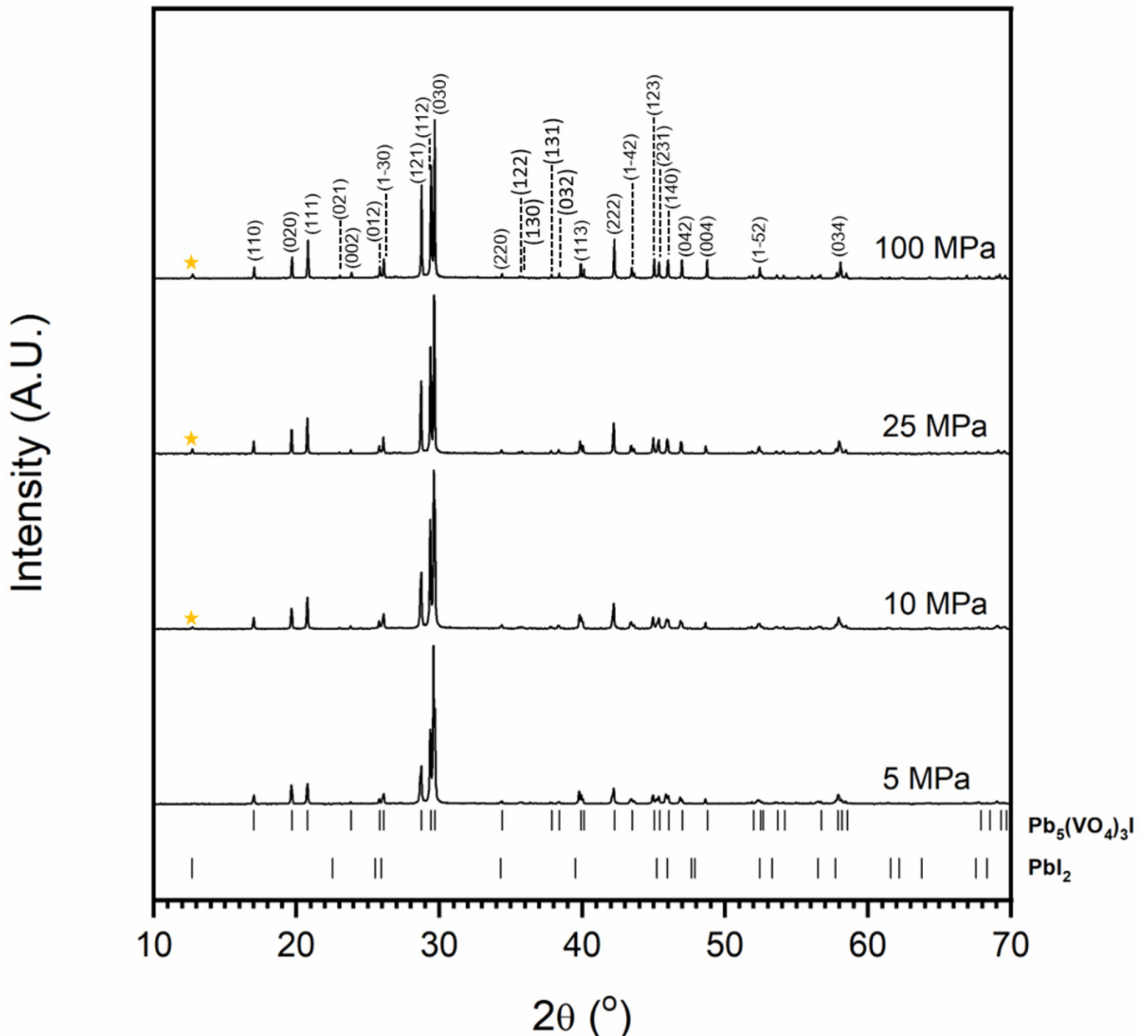


Figure 1. Powder X-ray diffraction profiles of iodovanadinite (labelled (hkl) Miller indices) synthesised with varying overpressure. The orange star indicates major PbI_2 peak. Tick marks show major reflections of $Pb_5(VO_4)_3I$ (ICSD 280065) and PbI_2 (ICSD 42013).

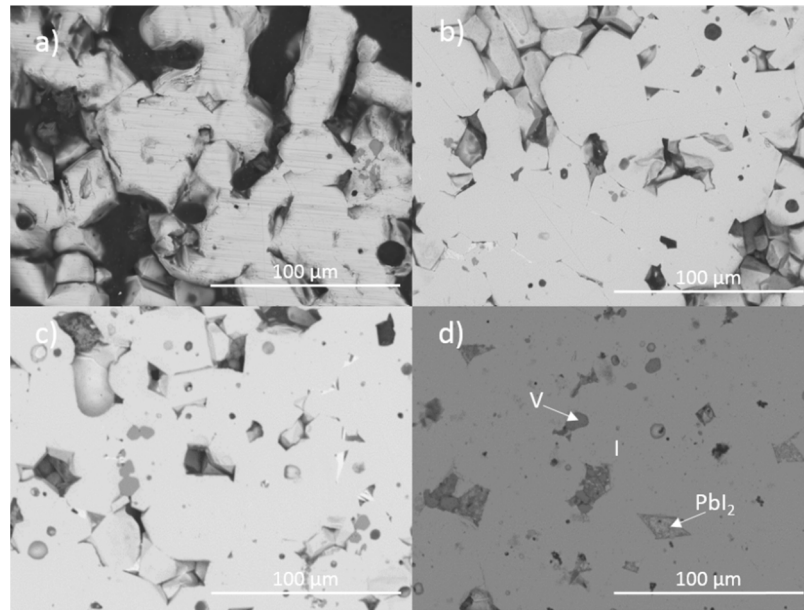


Figure 2. Representative backscattered electron micrographs of $\text{Pb}_5(\text{VO}_4)_3\text{I}$ consolidated with differing overpressures: (a) 5 MPa, (b) 10 MPa, (c) 25 MPa and (d) 100 MPa. I = iodovanadinite, V = V_2O_5 .

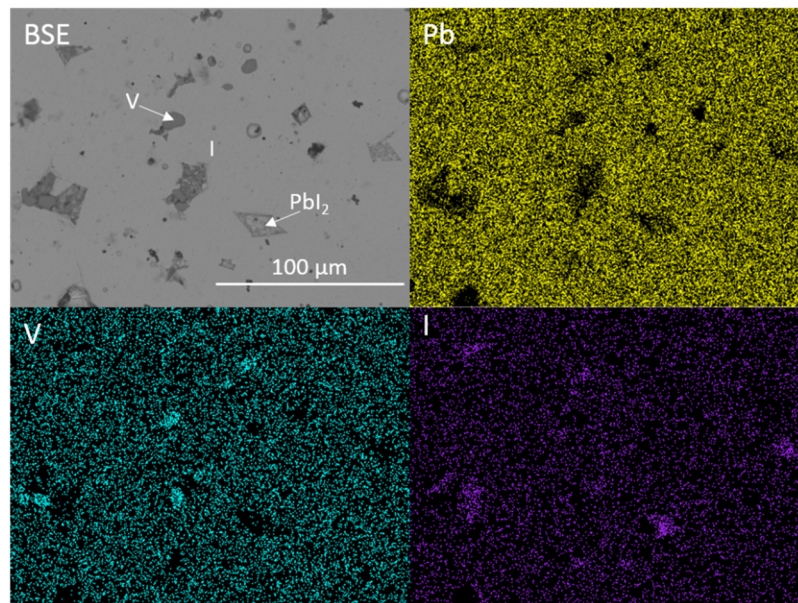


Figure 3. BSE micrograph and accompanying EDX maps displaying the microstructure and elemental distribution of Pb, V and I in baseline $\text{Pb}_5(\text{VO}_4)_3\text{I}$. I = iodovanadinite, V = V_2O_5 .

3.2. $\text{Pb}_{5-x}\text{Ag}_x(\text{VO}_4)_{3-x}(\text{MoO}_4)_x\text{I}$ Series

Figure 4 shows the results of X-ray diffraction for attempted syntheses in the $\text{Pb}_{5-x}\text{Ag}_x(\text{VO}_4)_{3-x}(\text{MoO}_4)_x\text{I}$ series; the unit cell parameters of the synthesised iodovanadinite phase are given in Table 1. As can be seen in Figure 4, even low levels of substitution, e.g., $x = 0.2$, resulted in the formation of secondary phases and the absence of the target iodovanadinite phase above $x = 0.6$. Observed secondary phases were PbI_2 , PbMoO_4 , $\text{Pb}_3(\text{VO}_4)_2$ and AgI . It is evident that increasing substitution of Mo led to increased formation of the PbMoO_4 phase. The incorporation of AgI was also limited, as can be seen by the increasing intensity of the associated reflections in the XRD profile.

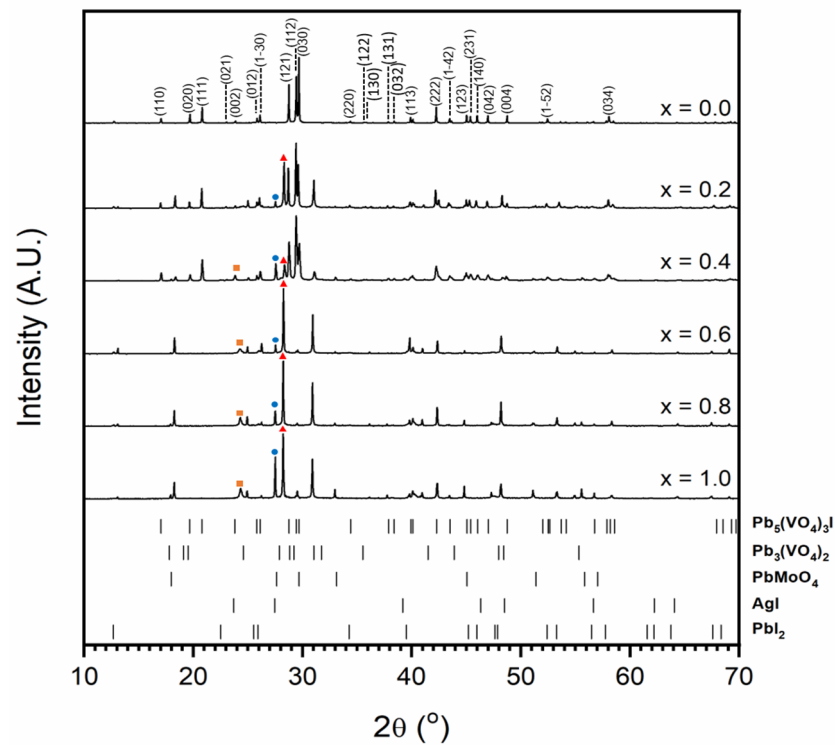


Figure 4. Powder X-ray diffraction profiles of synthesised iodovanadinite (labelled (hkl) Miller indices) and attempted syntheses in the $\text{Pb}_{5-x}\text{Ag}_x(\text{VO}_4)_{3-x}(\text{MoO}_4)_x\text{I}$ series. The orange square, blue circle and red triangle indicate major AgI , PbMoO_4 and $\text{Pb}_3(\text{VO}_4)_2$ peaks, respectively. Tick marks show major reflections for $\text{Pb}_5(\text{VO}_4)_3\text{I}$ (ICSD 280065), $\text{Pb}_3(\text{VO}_4)_2$ (ICSD 29360), PbMoO_4 (ICSD 164725), AgI (ICSD 164959) and PbI_2 (ICSD 42013). The minimum intensity of tick marks shown is 2% of their maximum intensity.

Table 1. Unit cell parameters of iodovanadinite phase in the $\text{Pb}_{5-x}\text{Ag}_x(\text{VO}_4)_{3-x}(\text{MoO}_4)_x\text{I}$ series. The iodovanadinite phase did not form for $x \geq 0.6$.

Target Composition	a (Å)	c (Å)
$\text{Pb}_5(\text{VO}_4)_3\text{I}$	10.4530 (1)	7.4822 (1)
$\text{Pb}_{4.8}\text{Ag}_{0.2}(\text{VO}_4)_{2.8}(\text{MoO}_4)_{0.2}\text{I}$	10.4695 (2)	7.4816 (2)
$\text{Pb}_{4.6}\text{Ag}_{0.4}(\text{VO}_4)_{2.6}(\text{MoO}_4)_{0.4}\text{I}$	10.464 (1)	7.483 (1)
$\text{Pb}_{4.4}\text{Ag}_{0.6}(\text{VO}_4)_{2.4}(\text{MoO}_4)_{0.6}\text{I}$	-	-
$\text{Pb}_{4.2}\text{Ag}_{0.8}(\text{VO}_4)_{2.2}(\text{MoO}_4)_{0.8}\text{I}$	-	-
$\text{Pb}_{4.0}\text{Ag}_{1.0}(\text{VO}_4)_{2.0}(\text{MoO}_4)_{1.0}\text{I}$	-	-

Figure 5 shows the backscattered electron (BSE) image of the targeted iodovanadinite composition $\text{Pb}_4\text{Ag}(\text{VO}_4)_2(\text{MoO}_4)\text{I}$. Comparing Figures 3 and 5, the coupled Pb/Ag and V/Mo substitution led to the retention of AgI and the formation of PbMoO_4 and $\text{Pb}_3(\text{VO}_4)_2$ instead of the desired iodovanadinite.

When PbI_2 was used as the major iodine source, although small inclusions of unreacted PbI_2 were identified in the final sample, iodine incorporation into the iodovanadinite phase was observed. Conversely, when AgI was used as the major iodine source, the iodovanadinite phase was not observed, and instead, the iodine remained as AgI inclusions found between grains of the PbMoO_4 and $\text{Pb}_3(\text{VO}_4)_2$ phases. It is noted that Klement and Harth (1962) found that $\text{Pb}_3(\text{VO}_4)_2$ did not react with NaI to form an iodovanadinite, whereas reactions with NaCl and NaBr yielded the corresponding chloro- and bromovanadinite phases [28]. This would suggest that halovanadinite formation is sensitive to which precursor is used, and therefore the immobilisation of I sequestered in AgI may benefit from an intermediate processing step to produce a more suitable precursor (such as PbI_2).

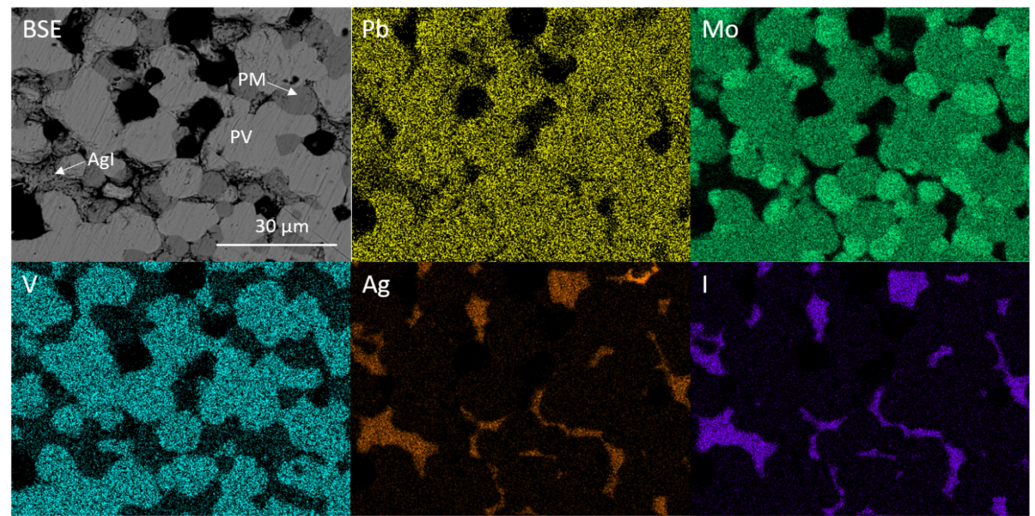


Figure 5. BSE micrograph and corresponding EDX maps displaying elemental distribution of Pb, Mo, V, Ag and I for targeted $\text{Pb}_4\text{Ag}(\text{VO}_4)_2(\text{MoO}_4)\text{I}$. PV = $\text{Pb}_3(\text{VO}_4)_2$, PM = PbMoO_4 .

The overlap of the Pb $M\alpha$ and Mo $L\alpha$ emission lines (2.3423 and 2.2921 keV, respectively) makes it difficult to discern whether Mo is incorporated into both $\text{Pb}_3(\text{VO}_4)_2$ and PbMoO_4 by study of elemental maps (Figure 5). However, it is apparent from the contrast in backscattered electron images that two Pb-bearing phases exist, and closer inspection of EDX point spectra reveals that a negligible amount of Mo was incorporated in the $\text{Pb}_3(\text{VO}_4)_2$ phase, due to the absence of characteristic X-ray emission below ~ 2.3 keV (see Figure 6). Regarding the formation of secondary PbMoO_4 , Porter et al. (2004) studied the durability of several Pb mineral phases over a wide pH range and found that the solubility of PbMoO_4 was comparable to pyromorphite $\text{Pb}_5(\text{PO}_4)_3\text{Cl}$, an apatite phase isostructural to the target iodovanadinite phase, at $\text{pH} > 7$ and superior at $\text{pH} < 7$ [29]. This may indicate that, although PbMoO_4 is formed as an accessory phase, it could, hypothetically, act as a suitable host phase for technetium in a multiphase wasteform with suitable charge compensation. Indeed, we note that Tc-99m may be isolated from solution by quantitative co-precipitation with PbMoO_4 [30].

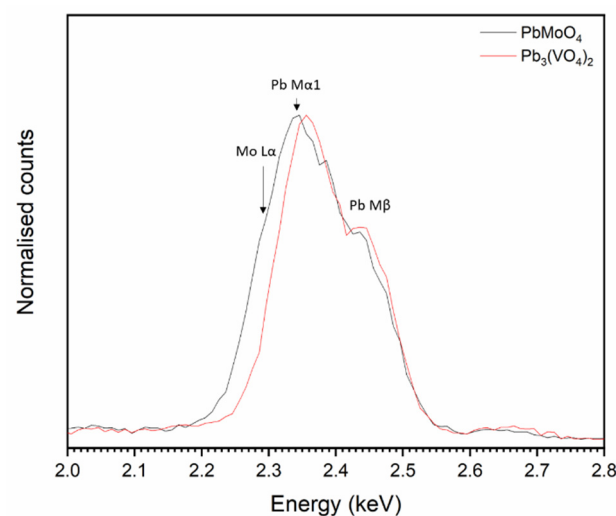


Figure 6. Normalised, summed EDX data taken from point spectra of PbMoO_4 and $\text{Pb}_3(\text{VO}_4)_2$ grains.

Figure 7 shows the results of coupled thermogravimetric analysis and mass spectrometry for the $\text{Pb}_{5-x}\text{Ag}_x(\text{VO}_4)_{3-x}(\text{MoO}_4)_x\text{I}$ series. For all compositions, an initial weight loss was observed, followed by a larger weight loss, which can be associated with the

loss of iodine; an intermediate weight loss step was also observed in samples containing greater amounts of PbI_2 ($x = 0-0.6$). Mass spectrometry of evolved gases was consistent with both monatomic and diatomic iodine (127 and 254 atomic mass units, respectively) being evolved with increasing temperature. It is apparent that, when PbI_2 was used as the iodine source, mass loss was far greater under these conditions, as can be seen in Figure 7a between 390 and 800 °C in the mass spectrum. This mass loss equates to ~ 8.9 wt%, a value comparable with the theoretical maximum iodine loading of 8.4 wt%, indicating complete iodine loss. These results are comparable to those reported by Stennett et al. (2011) and Lu et al. (2014) [18,21]. Samples containing a greater proportion of AgI were found to lose less iodine as a result of the greater thermal stability of AgI (m.p. = 558 °C) relative to PbI_2 (m.p. = 402 °C) e.g., mass loss observed for $\text{Pb}_4\text{Ag}(\text{VO}_4)_2(\text{MoO}_4)\text{I}$ (made using AgI as the sole iodine source) was only 1.19 wt% over the same temperature range. Although PbI_2 and AgI are both molten at temperatures greater than 558 °C, a proportion of iodine is retained within the melt and is liberated at higher temperatures, as indicated by the release of iodine at temperatures above the melting point of either precursor. From these results, it is clear that any processing of iodovanadinite wasteforms would benefit from the use of a closed system such as a HIP, especially those using a PbI_2 precursor.

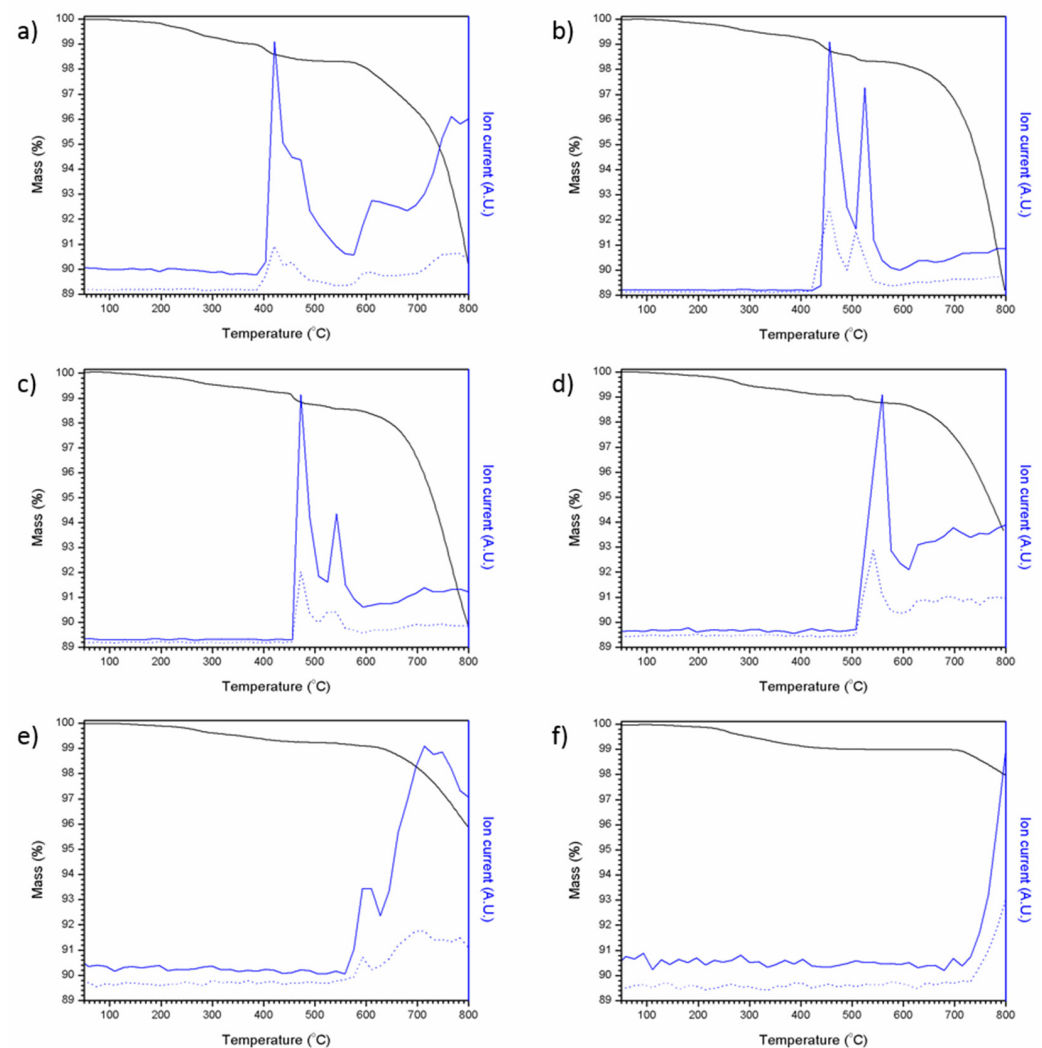


Figure 7. TGA-MS results for attempted $\text{Pb}_{5-x}\text{Ag}_x(\text{VO}_4)_{3-x}(\text{MoO}_4)_x\text{I}$ syntheses: (a) $x = 0.0$, (b) $x = 0.2$, (c) $x = 0.4$, (d) $x = 0.6$, (e) $x = 0.8$ and (f) $x = 1.0$. Ion current values are normalised, solid blue line = 127 AMU and dotted blue line = 254 AMU, black line = mass %.

3.3. $Pb_{4.5-x}Ba_xAg_{0.5}(VO_4)_3I_{0.5}$ Series

Figure 8 shows the X-ray diffraction patterns observed for the results of attempted syntheses of the $Pb_{4.5-x}Ba_xAg_{0.5}(VO_4)_3I_{0.5}$ series. Phase-pure iodovanadinite is not formed for any composition in the series. Instead, substitution of Ba for Pb results in the formation of $Ba_3(VO_4)_2$ structured material at levels as low as $x = 0.5$ formula units. The shift in the position of major XRD reflections with increasing Ba substitution is indicative of solid solution behaviour between Pb and Ba in the $Ba_3(VO_4)_2$ structure. This is supported by the refined unit cell parameters and EDX spot analyses (Table 2) that show linear variation in the Pb:Ba ratio and that, as Ba content increases, unit cell size increases. This is as expected, given the larger ionic radius of Ba relative to Pb ($r_{Ba} = 1.52 \text{ \AA}$ and 1.61 \AA , and $r_{Pb} = 1.4 \text{ \AA}$ and 1.49 \AA , in 10 and 12-fold co-ordination, respectively). Further SEM-EDX analyses of sectioned HIP samples supported the results of XRD. Grains of reacted vanadate material separated by unreacted AgI were observed (Figures 9–11). The interconnected AgI affected the sintering of the vanadate material, resulting in poorly consolidated material that is prone to pulling-out during polishing, as can be seen in the BSE images.

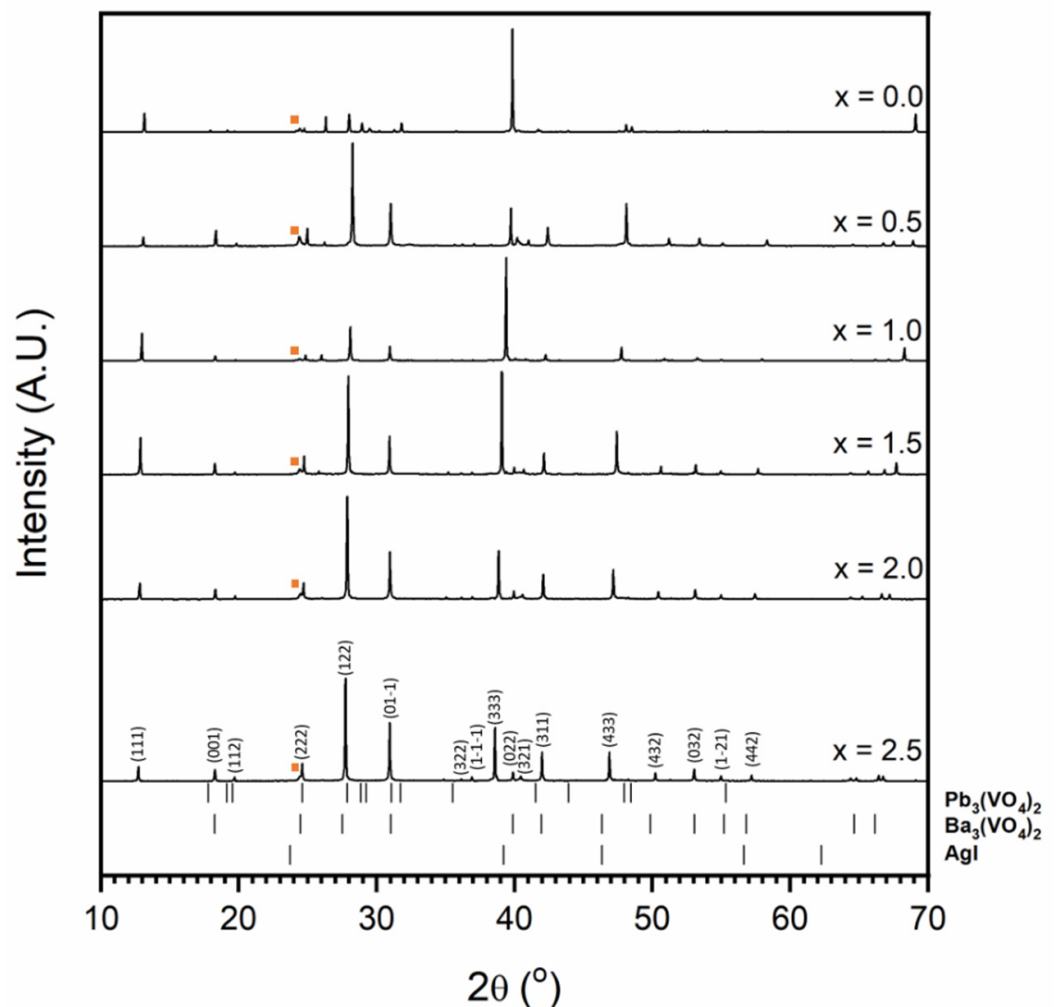


Figure 8. Powder diffraction patterns for materials resulting from attempted syntheses in the $Pb_{4.5-x}Ba_xAg_{0.5}(VO_4)_3I_{0.5}$ series. The orange square indicates major AgI peak. Tick marks show allowed major reflections for $Pb_3(VO_4)_2$ (ICSD 29360), $Ba_3(VO_4)_2$ (labelled (hkl) Miller indices; ICSD 14237) and AgI (ICSD 164959). The minimum intensity of tick marks shown is 2% of their maximum intensity.

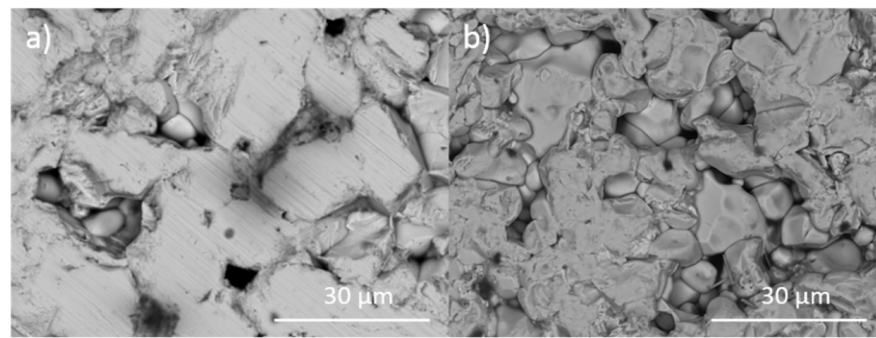


Figure 9. Representative backscattered electron images of targeted iodovanadinites in the $\text{Pb}_{4.5-x}\text{Ba}_x\text{Ag}_{0.5}(\text{VO}_4)_3\text{I}_{0.5}$ series: (a) $\text{Pb}_{4.5}\text{Ag}_{0.5}(\text{VO}_4)_3\text{I}_{0.5}$ and (b) $\text{Pb}_2\text{Ba}_{2.5}\text{Ag}_{0.5}(\text{VO}_4)_3\text{I}_{0.5}$.

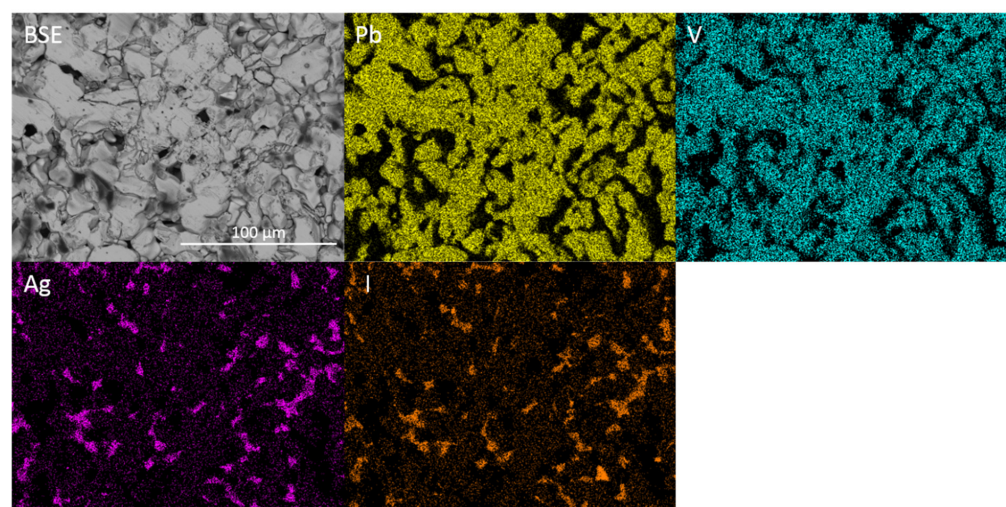


Figure 10. BSE image and corresponding EDX maps displaying elemental distribution of Pb, V, Ag and I for target stoichiometry $\text{Pb}_{4.5}\text{Ag}_{0.5}(\text{VO}_4)_3\text{I}_{0.5}$.

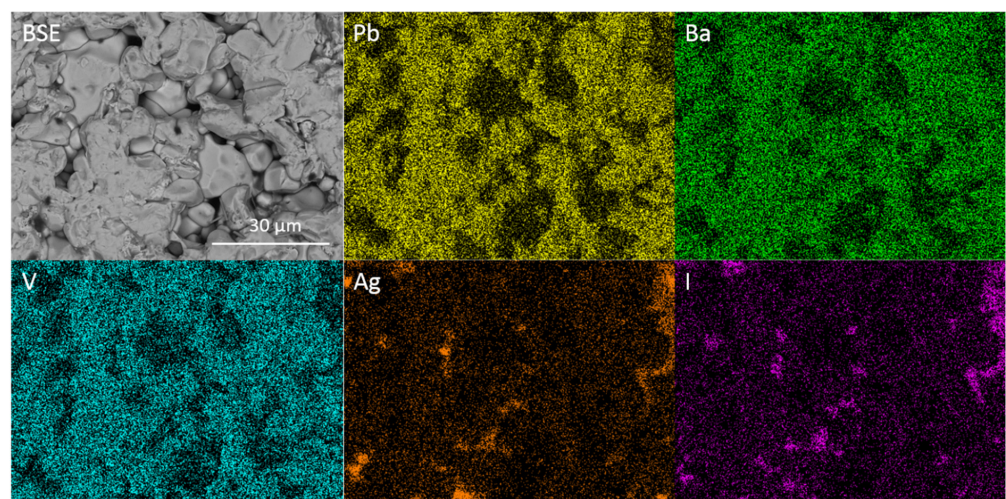


Figure 11. BSE image of microstructure and corresponding EDX maps displaying elemental distribution of Pb, Ba, V, Ag and I for target stoichiometry $\text{Pb}_2\text{Ba}_{2.5}\text{Ag}_{0.5}(\text{VO}_4)_3\text{I}_{0.5}$.

These results are similar to those of Klement and Harth, who found that barium vanadate did not react with molten NaI or NaBr and remained as $\text{Ba}_3(\text{VO}_4)_2$, whereas reaction with molten NaCl yielded the vanadinite phase [31]. Johnstone et al. attempted the synthesis of $\text{AgPb}_9(\text{VO}_4)_6\text{I}$ and the $\text{AgBa}_9(\text{VO}_4)_6\text{I}$ phase described by Uno et al. using

AgI, $\text{Pb}_3(\text{VO}_4)_2$ and $\text{Ba}_3(\text{VO}_4)_2$ precursors [26], but showed that these compounds cannot be isolated; synthesis under the reported conditions yields a mixture of AgI and $\text{Ba}_3(\text{VO}_4)_2$ or $\text{Pb}_3(\text{VO}_4)_2$. Similarly, in the present study, AgI was found to not react with vanadate phases irrespective of vanadate phase stoichiometry, and variation in Pb/Ba stoichiometry did not improve the final phase assemblage. Maddrell and Abruatis found it was possible to synthesise single-phase $\text{Pb}_{4.5}\text{Ba}_{0.5}(\text{VO}_4)_3\text{I}$, indicating that it is likely that the use of AgI as the iodine source has affected the formation of the iodovanadinite phase, and it may be possible to synthesise Ba-containing iodovanadinite if a different precursor is used [23]. In this context, it is worth noting that the synthesis of $\text{Pb}_5(\text{VO}_4)_3\text{I}$ was successfully achieved using PdI_2 as a sacrificial iodine source, relevant to the direct immobilisation of undissolved PdI_2 residues formed in nuclear fuel reprocessing [32].

Figure 12 shows the results of coupled thermogravimetric analysis and mass spectrometry for the $\text{Pb}_{4.5-x}\text{Ba}_x\text{Ag}_{0.5}(\text{VO}_4)_3\text{I}_{0.5}$ series. The results of TGA-MS were very similar to those observed for $\text{Pb}_4\text{Ag}(\text{VO}_4)_2(\text{MoO}_4)\text{I}$ (AgI used as the sole iodine source). An initial weight loss was followed by a plateau from ~ 500 – 700 °C and then a second weight loss in association with the evolution of monatomic and diatomic iodine. In the case of target compositions $x = 2.0$ and $x = 2.5$, the corresponding MS data, Figure 12e,f, respectively, did not evidence a signal associated with the evolution of monatomic and diatomic iodine but are consistent with the background signal observed for compositions $x = 0.0, 0.5$ and 1.0 (Figure 12a–c). This was due to iodine plating out in the TGA-MS transfer line in the case of compositions $x = 1.5$ and $x = 2.0$, as a result of a drop in temperature.

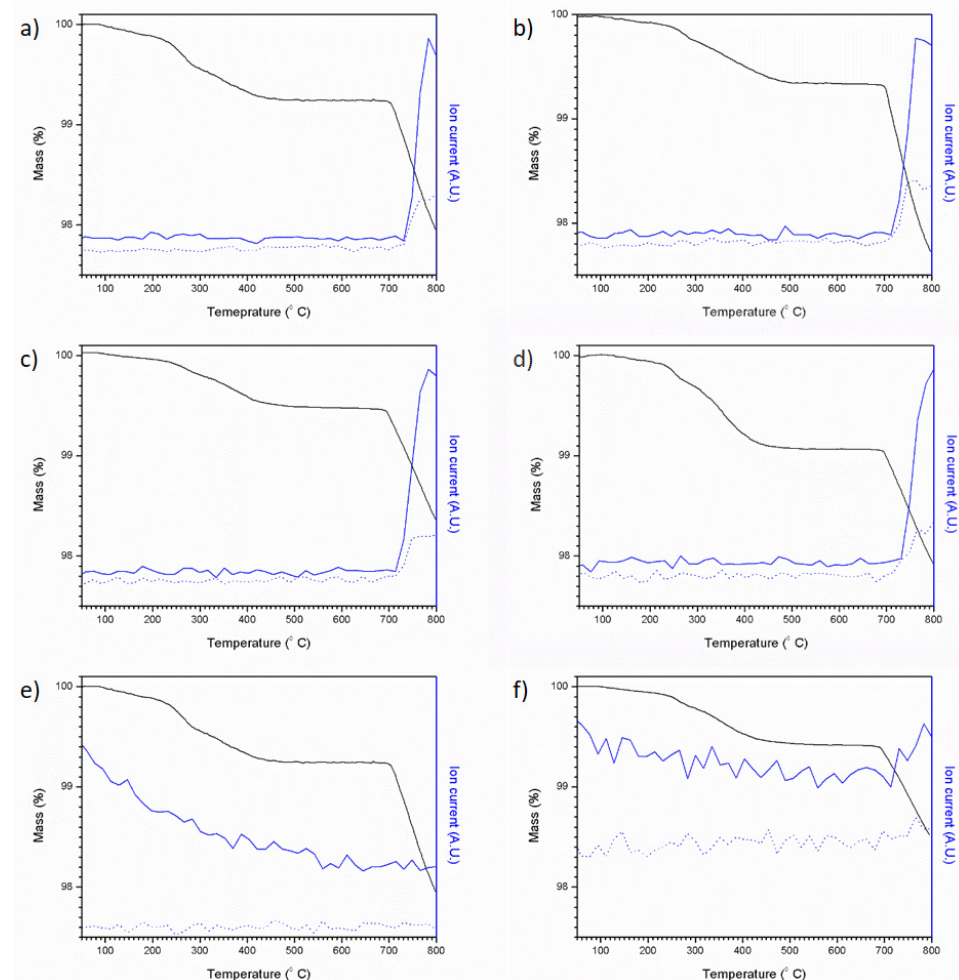


Figure 12. TGA-MS results for attempted $\text{Pb}_{4.5-x}\text{Ba}_x\text{Ag}_{0.5}(\text{VO}_4)_3\text{I}_{0.5}$ syntheses: (a) $x = 0.0$, (b) $x = 0.5$, (c) $x = 1.0$, (d) $x = 1.5$, (e) $x = 2.0$ and (f) $x = 2.5$. Ion current values are normalised, solid blue line = 127 AMU and dotted blue line = 254 AMU, black line = mass %.

Table 2. Refined unit cell parameters of Ba₃(VO₄)₂ structured phase.

Target Composition	Ba ₃ (VO ₄) ₂ Phase EDX Composition	a (Å)	α (°)
Pb _{4.5} Ag _{0.5} (VO ₄) ₃ I _{0.5}	Pb _{2.96±0.15} Ag _{0.04±0.06} (VO ₄) _{2.24±0.17} I _{0.06±0.05}	-	-
Pb _{4.0} Ba _{0.5} Ag _{0.5} (VO ₄) ₃ I _{0.5}	Pb _{2.55±0.09} Ba _{0.44±0.04} Ag _{0.01±0.02} (VO ₄) _{2.08±0.06} I _{0.03±0.04}	7.590 (2)	44.756 (8)
Pb _{3.5} Ba _{0.5} Ag _{0.5} (VO ₄) ₃ I _{0.5}	Pb _{2.16±0.13} Ba _{0.75±0.33} Ag _{0.1±0.05} (VO ₄) _{1.39±0.32} I _{0.03±0.03}	7.642 (1)	44.525 (7)
Pb _{3.0} Ba _{1.5} Ag _{0.5} (VO ₄) ₃ I _{0.5}	Pb _{1.94±0.13} Ba _{0.99±0.05} Ag _{0.07±0.06} (VO ₄) _{1.81±0.18} I _{0.01±0.02}	7.689 (1)	44.259 (5)
Pb _{2.5} Ba _{2.0} Ag _{0.5} (VO ₄) ₃ I _{0.5}	Pb _{1.69±0.27} Ba _{1.24±0.14} Ag _{0.07±0.06} (VO ₄) _{1.92±0.24} I _{0.03±0.04}	7.733 (1)	44.010 (6)
Pb _{2.0} Ba _{2.5} Ag _{0.5} (VO ₄) ₃ I _{0.5}	Pb _{1.30±0.08} Ba _{1.63±0.09} Ag _{0.07±0.05} (VO ₄) _{1.78±0.07} I _{0.01±0.02}	7.769 (1)	43.771 (5)

4. Conclusions

The potential for co-immobilisation of I and Tc in iodovanadinites derived from Pb₅(VO₄)₃I was investigated in the hypothetical systems Pb_{5-x}Ag_x(VO₄)_{3-x}(MoO₄)_xI and Pb_{4.5-x}Ba_xAg_{0.5}(VO₄)₃I_{0.5}, using Mo as a Tc surrogate. Solid-state synthesis utilised a closed system and hot isostatic pressing to prevent iodine volatilisation. Importantly, the direct synthesis of Pb₅(VO₄)₃I by hot isostatic pressing was proven successfully for the first time, utilising PbI₂ as an iodine source. The HIP overpressure does not strongly influence the phase assemblage, but a higher pressure of 100 MPa proved optimal for achieving a ceramic microstructure with negligible inter-granular porosity and near single-phase Pb₅(VO₄)₃I. Synthesis of Pb_{5-x}Ag_x(VO₄)_{3-x}(MoO₄)_xI iodovanadinites proved unsuccessful, with even a low level of substitution (x = 0.2) resulting in the formation of secondary phases PbI₂, PbMoO₄, Pb₃(VO₄)₂ and AgI. Likewise, the synthesis of the Pb_{4.5-x}Ba_xAg_{0.5}(VO₄)₃I_{0.5} iodovanadinites proved unsuccessful; the products comprised an apparently novel (Ba,Pb)₃(VO₄)₂ solid solution plus AgI. The use of AgI as an iodine source was found to be problematic, with negligible incorporation into the target iodovanadinite phase observed. Although this investigation did not successfully demonstrate co-immobilisation of I and Tc in the iodovanadinite structure, with Mo as a Tc surrogate, the approach may have some merit for further development, targeting a composite Pb₅(VO₄)₃I–PbMoO₄ ceramic, given that PbMoO₄ has been shown to incorporate Tc. Nevertheless, this work has taken an important step forward in demonstrating the first direct synthesis of Pb₅(VO₄)₃I as a wasteform for I-129 by hot isostatic pressing.

Author Contributions: Conceptualization, D.J.B. and N.C.H.; Methodology, D.J.B. and N.C.H.; Formal analysis, D.J.B., E.V.J., M.C.S. and N.C.H.; Investigation, D.J.B., E.V.J., M.C.S. and C.L.C.; Writing—original draft, D.J.B.; Writing—review and editing, D.J.B., E.V.J. and N.C.H.; Supervision, E.V.J., M.C.S., C.L.C. and N.C.H.; Funding acquisition, N.C.H. and C.L.C. All authors have read and agreed to the published version of the manuscript.

Funding: We are grateful to EPSRC (Engineering and Physical Sciences Research Council) for sponsoring this research under grant references EP/M026566/1, EP/S032959/1, EP/S011935/1 and EP/S01019X/1. NCH is grateful to the Royal Academy of Engineering and the Nuclear Decommissioning Authority for the partial sponsorship of this research. CLC is grateful to EPSRC for the award of an Early Career Fellowship under grant reference EP/N017374/1. The research reported here was performed at the MIDAS/HADES Facility at the University of Sheffield, which was established with support from the DECC/BEIS and EPSRC under grant reference EP/T011424/1 [33].

Data Availability Statement: The raw data that supports these findings cannot be shared at this time as the data also form part of an ongoing study.

Conflicts of Interest: The authors declare that they have no known competing financial interest or personal relationships that could have appeared to influence the work reported in this paper.

References

1. Wilson, P.D. *The Nuclear Fuel Cycle: From Ore to Waste*; Oxford University Press: Oxford, UK, 1996.
2. Riley, B.J.; Vienna, J.D.; Strachan, D.M.; McCloy, J.S.; Jerden, J.L., Jr. Materials and processes for the effective capture and immobilization of radioiodine: A review. *J. Nucl. Mater.* **2016**, *470*, 307–326. [[CrossRef](#)]

3. O'Sullivan, S.E.; Montoya, E.; Sun, S.K.; George, J.; Kirk, C.; Dixon Wilkins, M.C.; Weck, P.F.; Kim, E.; Knight, K.S.; Hyatt, N.C. Crystal and electronic structures of A_2NaIO_6 periodate double perovskites ($A = Sr, Ca, Ba$): Candidate wasteforms for I-129 immobilization. *Inorg. Chem.* **2020**, *59*, 18407–18419. [[CrossRef](#)]
4. Asmussen, R.M.; Turner, J.; Chong, S.; Riley, B.J. Review of recent developments in iodine wasteform production. *Front. Chem.* **2022**, *10*, 1043653. [[CrossRef](#)] [[PubMed](#)]
5. Umadevi, K.; Mandal, D. Performance of radio-iodine discharge control methods of nuclear reprocessing plants. *J. Environ. Radioact.* **2021**, *234*, 106623. [[CrossRef](#)] [[PubMed](#)]
6. Buck, E.C.; Mausolf, E.J.; McNamara, B.K.; Soderquist, C.Z.; Schwantes, J.M. Sequestration of radioactive iodine in silver-palladium phases in commercial spent nuclear fuel. *J. Nucl. Mater.* **2016**, *482*, 229–235. [[CrossRef](#)]
7. Chapman, K.W.; Chupas, P.J.; Nenoff, T.M. Radioactive iodine capture in silver-containing mordenites through nanoscale silver iodide formation. *J. Am. Chem. Soc.* **2010**, *132*, 8897–8899. [[CrossRef](#)]
8. Olsen, Y.S.; i Batlle, J.V. A model for the bioaccumulation of ^{99}Tc in lobsters (*Homarus gammarus*) from the West Cumbrian coast. *J. Environ. Radioact.* **2003**, *67*, 219–233. [[CrossRef](#)]
9. Donald, I.W. *Waste Immobilization in Glass and Ceramic Based Hosts: Radioactive, Toxic and Hazardous Wastes*; John Wiley & Sons: Hoboken, NJ, USA, 2010.
10. Schwochau, K. *Technetium: Chemistry and Radiopharmaceutical Applications*; John Wiley & Sons: Hoboken, NJ, USA, 2008.
11. Poineau, F.; Du Mazaubrun, J.; Ford, D.; Fortner, J.; Kropf, J.; Silva, G.C.; Smith, N.; Long, K.; Jarvinen, G.; Czerwinski, K.R. Uranium/technetium separation for the UREX process—synthesis and characterization of solid reprocessing forms. *Radiochim. Acta* **2008**, *96*, 527–533. [[CrossRef](#)]
12. Audubert, F.; Carpena, J.; Lacout, J.L.; Tetard, F. Elaboration of an iodine-bearing apatite iodine diffusion into a $Pb_3(VO_4)_2$ matrix. *Solid State Ionics* **1997**, *95*, 113–119. [[CrossRef](#)]
13. White, T.J.; d Dong, Z. Structural derivation and crystal chemistry of apatites. *Acta Crystallogr. B Struct. Sci. Cryst. Eng. Mater.* **2003**, *59*, 1–16. [[CrossRef](#)]
14. Schriewer, M.S.; Jeitschko, W. Preparation and crystal structure of the isotypic orthorhombic strontium perrhenate halides $Sr_5(ReO_5)_3X$ ($X = Cl, Br, I$) and structure refinement of the related hexagonal apatite-like compound $Ba_5(ReO_5)_3Cl$. *J. Solid State Chem.* **1993**, *107*, 1–11. [[CrossRef](#)]
15. Audubert, F.; Savariault, J.M.; Lacout, J.L. Pentalead tris (vanadate) iodide, a defect vanadinite-type compound. *Acta Crystallogr. C Struct. Chem.* **1999**, *55*, 271–273. [[CrossRef](#)]
16. Baud, G.; Besse, J.P.; Sueur, G.; Chevalier, R. Structure de nouvelles apatites au rhenium contenant des anions volumineux: $Ba_{10}(ReO_5)_6X_2$ ($X = Br, I$). *Mater. Res. Bull.* **1979**, *14*, 675–682. [[CrossRef](#)]
17. Le Gallet, S.; Campayo, L.; Courtois, E.; Hoffmann, S.; Grin, Y.; Bernard, F.; Bart, F. Spark plasma sintering of iodine-bearing apatite. *J. Nucl. Mater.* **2010**, *400*, 251–256. [[CrossRef](#)]
18. Stennett, M.C.; Pinnock, I.J.; Hyatt, N.C. Rapid synthesis of $Pb_5(VO_4)_3I$, for the immobilisation of iodine radioisotopes, by microwave dielectric heating. *J. Nucl. Mater.* **2011**, *414*, 352–359. [[CrossRef](#)]
19. Redfern, S.A.T.; Smith, S.E.; Maddrell, E.R. High-temperature breakdown of the synthetic iodine analogue of vanadinite, $Pb_5(VO_4)_3I$: An apatite-related compound for iodine radioisotope immobilization? *Miner. Mag.* **2012**, *76*, 997–1003. [[CrossRef](#)]
20. Suetsugu, Y. Synthesis of lead vanadate iodoapatite utilizing dry mechanochemical process. *J. Nucl. Mater.* **2014**, *454*, 223–229. [[CrossRef](#)]
21. Lu, F.; Yao, T.; Xu, J.; Wang, J.; Scott, S.; Dong, Z.; Ewing, R.C.; Lian, J. Facile low temperature solid state synthesis of iodoapatite by high-energy ball milling. *RSC Adv.* **2014**, *4*, 38718–38725. [[CrossRef](#)]
22. Zhang, M.; Maddrell, E.R.; Abraitis, P.K.; Salje, E.K.H. Impact of leach on lead vanado-iodoapatite [$Pb_5(VO_4)_3I$]: An infrared and Raman spectroscopic study. *Mater. Sci. Eng. B Solid State Mater. Adv. Technol.* **2007**, *137*, 149–155. [[CrossRef](#)]
23. Maddrell, E.R.; Abraitis, P.K. A comparison of wasteforms and processes for the immobilisation of iodine-129. *MRS Proc.* **2003**, *807*, 565–570. [[CrossRef](#)]
24. Guy, C.; Audubert, F.; Lartigue, J.E.; Latrille, C.; Advocat, T.; Fillet, C. New conditionings for separated long-lived radionuclides. *Comptes Rendus Phys.* **2002**, *3*, 827–837. [[CrossRef](#)]
25. Uno, M.; Kosuga, A.; Masuo, S.; Imamura, M.; Yamanaka, S. Thermal and mechanical properties of $AgPb_9(VO_4)_6I$ and $AgBa_9(VO_4)_6I$. *J. Alloys Compd.* **2004**, *384*, 300–302. [[CrossRef](#)]
26. Johnstone, E.V.; Bailey, D.J.; Stennett, M.C.; Heo, J.; Hyatt, N.C. On the existence of $AgM_9(VO_4)_6I$ ($M = Ba, Pb$). *RSC Adv.* **2017**, *7*, 49004–49009. [[CrossRef](#)]
27. Yao, T.; Lu, F.; Sun, H.; Wang, J.; Ewing, R.C.; Lian, J. Bulk iodoapatite ceramic densified by spark plasma sintering with exceptional thermal stability. *J. Am. Ceram. Soc.* **2014**, *97*, 2409–2412. [[CrossRef](#)]
28. Klement, R.; Harth, R. Über Bleiapatite und tertiäres Bleiphosphat. *Z. Für Anorg. Allg. Chem.* **1962**, *314*, 238–244. [[CrossRef](#)]
29. Porter, S.K.; Scheckel, K.G.; Impellitteri, C.A.; Ryan, J.A. Toxic metals in the environment: Thermodynamic considerations for possible immobilization strategies for Pb, Cd, As, and Hg. *Crit. Rev. Environ. Sci. Technol.* **2004**, *34*, 495–604. [[CrossRef](#)]
30. Ichikawa, F. The isolation of technetium by coprecipitation or anion exchange. *Bull. Chem. Soc. Jpn.* **1959**, *32*, 1126–1129. [[CrossRef](#)]
31. Klement, R.; Harth, R. Das Verhalten von tertiären Erdalkaliphosphaten, -arsenaten und -vanadaten in geschmolzenen Halogeniden. *Chem. Ber.* **1961**, *94*, 1452–1456. [[CrossRef](#)]

32. Johnstone, E.V.; Bailey, D.J.; Lawson, S.; Stennett, M.C.; Corkhill, C.L.; Kim, M.; Heo, J.; Matsumura, D.; Hyatt, N.C. Synthesis and characterization of iodovanadinite using PdI₂, an iodine source for the immobilisation of radioiodine. *RSC Adv.* **2020**, *10*, 25116–25124. [[CrossRef](#)]
33. Hyatt, N.C.; Corkhill, C.L.; Stennett, M.C.; Hand, R.J.; Gardner, L.J.; Thorpe, C.L. The HADES facility for high activity decommissioning engineering & science: Part of the UK national nuclear user facility. *IOP Conf. Ser. Mater. Sci.* **2020**, *818*, 012022.

Disclaimer/Publisher's Note: The statements, opinions and data contained in all publications are solely those of the individual author(s) and contributor(s) and not of MDPI and/or the editor(s). MDPI and/or the editor(s) disclaim responsibility for any injury to people or property resulting from any ideas, methods, instructions or products referred to in the content.